Published in final edited form as:
Ophthalmic Genet. 2010 September ; 31(3): 114–125. doi:10.3109/13816810.2010.482555.

Long-term 12 year follow-up of X-linked congenital retinoschisis

Sten Kjellström[1], **Camasamudram Vijayasarathy**[2], **Vesna Ponjavic**[1], **Paul A. Sieving**[3], and **Sten Andréasson**[1]

[1]Department of Ophthalmology, Lund University, Lund, Sweden [2]National Institutes on Deafness and Other Communication Disorders, National Institutes of Health, Bethesda, Maryland [3]National Eye Institute, National Institutes of Health, Bethesda, Maryland

Abstract

Purpose—To investigate the retinal structure and function during the progression of X-linked retinoschisis (XLRS) from childhood to adulthood.

Methods—Ten patients clinically diagnosed with XLRS were investigated at 6–15 years of age (mean age 9 years) with a follow-up 8 to 14 years later (mean 12 years). The patients underwent regular ophthalmic examination as well as testing of best corrected visual acuity (BCVA), visual field (VF) and assessment of full-field electroretinography (ERG) during their first visit. During the follow-up, the same clinical protocols were repeated. In addition, macular structure and function was examined with multifocal electroretinography (mfERG) and optical coherence tomography (OCT). The patients were 18–25 years of age (mean age 21 years) at the follow-up examination. All exons and exon-intron boundaries of *RS1*-gene were sequenced for gene mutations in 9 out of the 10 patients.

Results—Best corrected VA and VF were stable during this follow-up period. No significant progression in cone or rod function could be measured by full-field ERG. Multifocal electroretinography and OCT demonstrated a wide heterogeneity of macular changes in retinal structure and function at the time of follow-up visit. Three different mutations were detected in these nine patients, including a known nonsense mutation in exon 3, a novel insertion in exon 5 and an intronic mutation at 5' splice site of intron 3.

Conclusions—Clinical follow-up (mean 12 years) of ten young XLRS patients (mean age of 9 years) with a typical congenital retinoschisis phenotype revealed no significant decline in retinal function during this time period. MfERG and OCT demonstrated a wide variety of macular changes including structure and dysfunction. The XLRS disease was relatively stable during this period of observation and would afford opportunity for therapy studies to judge benefit against baseline and against the fellow eye.

Keywords

XLRS; genotype; phenotype; rate of progression

Correspondence: Dr. Sten Kjellström, Department of Ophthalmology, Lund University, S 221 85 Lund, Sweden. sten.kjellstrom@med.lu.se.

Declaration of interest: The authors report no conflict of interest. The authors alone are responsible for the content and writing of the paper.

INTRODUCTION

Juvenile retinoschisis is a genetic X-linked recessive retinal disease (XLRS) that affects 1:5000 to 1:25000 males worldwide and is one of the most common causes of juvenile macular degeneration in boys and adolescent men.[1] XLRS is a monogenic trait caused by mutations in the *RS1* gene.[2,3] Women who carry the trait rarely experience vision abnormality.

The *RS1* gene product, retinoschisin (RS1), is expressed in the retina[4] and pineal.5 It is a 24 kDa protein that encodes an evolutionarily conserved discoidin domain implicated in cell adhesion and signaling.6 Retinoschisin is predicted to serve as an adhesive protein in maintaining the structural and functional integrity of the retina.7 The condition manifests clinically with cystic changes in the macula which to some extent reduces visual acuity. Although the disease is congenital, most affected males are diagnosed about the time they reach school age because of failed vision tests. Visual acuity is frequently reduced to Snellen 0.2–0.4, but can be in the range from light perception to 0.9. In some severe cases with nystagmus, bilateral bullous schisis cavities and retinal detachment in the affected males are diagnosed at birth.

Clinical retinoschisis changes extend into the peripheral retina and cause lamellar splitting through multiple retinal planes, both in the nerve fiber layer at the retinal surface and also deeper in the retina. Peripheral retinoschisis occurs most commonly in the infero-temporal retina.8 The clinical literature indicates that about half of XLRS males have peripheral retinoschisis9 that leads to retinal lamellar holes with full thickness retinal detachment in up to 5–10% of cases. The recent introduction of optical coherence tomography (OCT) has increased the clinical sensitivity for detection,1 and a majority of XLRS males are found to have peripheral retinal involvement with schisis formations.11 Typical scotopic full-field electroretinography (ERG) findings in XLRS patients is a reduction of the b-wave response disproportionate to the a-wave,12 ie, a decrease in b/a-wave ratio. Furthermore there is often a delay in 30Hz flicker ERG implicit time.13–15

The clinical phenotype of XLRS is quite broad in the age and severity of clinical presentation and in the extent of peripheral retinal pathology.16 Visual deterioration, principally visual acuity loss, typically progresses during the first two decades of life. XLRS affected men often barely qualify for a drivers license (Sweden 0.5 Snellen). There is slow progression of severity into the fifth and sixth decades with an early onset age related macular degeneration that commonly causes additional visual failure.[8] XLRS patients over age 50 years frequently have macular pigmentary changes and / or retinal pigment epithelial (RPE) atrophy. The older age consequences have not been fully described, but in our clinical experience, visual failure can become profound even without complicating factors such as retinal detachment or vitreous hemorrhage, implicating a progressive failure and loss of retinal cells and function.

Macular changes seem to be present in almost all cases. In most young patients a wheel-like cystic formation is seen in the macula, whereas middle-aged and older patients more often present a non-specific atrophic appearance in the macula.

In this study we have examined clinically diagnosed XLRS patients from the Swedish Retinal Degeneration registry with different mutations in the XLRS1 gene in order to further evaluate the rate of progression.

METHODS

The study was conducted in accordance with the tenets of the Declaration of Helsinki and had the approval from the Ethics Committee, Lund University. Informed consent was obtained from each of the patients after they were provided sufficient information on the procedures to be used.

Patients

Male patients, from the Swedish RD-registry, a national registry of patients with retinal degeneration in Sweden containing approximate 2800 patients, between 18 and 25 years of age with clinical diagnosed congenital retinoschisis and with records of previous ophthalmologic examination including full-field ERG at least eight years earlier, were included in this study. The clinical diagnosis of X-linked retinoschisis was based on the ocular history, funduscopic findings, visual fields, ISCEV (International Society for Clinical Electrophysiology of Vision) standard full-field ERGs,[17] and in some cases OCT when available. Based on these inclusion criteria, 20 eyes of 10 patients with XLRS (10 males; mean age 21.4 years; range, 18–25) were included in this study. The first examination was conducted between ages 6 and 15 years (mean age 9.3 years), mean interval between examinations was 12.1 years (Table 1). All included patients were re-examined and underwent a complete ophthalmologic test including Snellen best corrected visual acuity (BCVA), full-field ERG, multifocal ERG, Goldmann visual field test, OCT and fundus photography. Blood was drawn for DNA analysis in 9 out of the 10 patients. Age matched controls for full-field ERG and mfERG responses were selected from a database of patients without signs of retinal degeneration using same standardized ERG protocols.

Full-field ERG

Full-field electroretinography (full field ERG) was recorded in a Nicolet analysis system (Nicolet Biomedical Instruments, Madison, WI, USA). The subjects were dark adapted for 40 minutes and a Burian Allen bipolar contact lens was applied on the cornea and a ground electrode on the forehead. Responses were obtained with a wide band filter (−3 dB at 1 Hz and 500 Hz) stimulating with brief (30 μs) single full-field flashes of dim blue light (Wratten filter #47, 47A and 47B) and white light (0.81 cd.s / m^2 and 3.93 cd.s / m^2). Cone responses were obtained with 30-Hz flickering white light (0.81 cd.s / m^2) averaged from 20 sweeps. If responses measuring less than 10 μV were recorded with single white flashes, recordings were also obtained with computer averaging (30 flashes), a bipolar artifact rejecter and a line frequency notch filter (50Hz). To obtain small cone responses, stimulation then included 200 sweeps of 30-Hz flickering white light and a digital or analogue narrow band-pass filter added to the system.

Multifocal ERG

Multifocal electroretinography (mfERG) was recorded using the visual evoked response imaging system (VERIS 4; EDI, San Mateo, CA, USA), developed by Sutter et al.[18, 19] The stimulus matrix consisted of 103 hexagonal elements displayed on a screen in the infrared (IR) camera. The recording procedures were performed according to the ISCEV guidelines for clinical mfERG.[20] Recordings were monocular and the fixation was controlled using the IR camera and illumination with infrared light from the recording electrode, with visualization of the hexagonal elements over the retina. The first order kernel P1 amplitudes and implicit times in ring areas 1–6 were calculated according to the guidelines for basic mfERG.[20] Responses from ring areas 1 and 2 were averaged, noted Ring (1 + 2).

Optical Coherence Tomography

OCT was performed on both eyes using the spectral domain 3D OCT-1000, version. 3.00 software (Topcon, Tokyo). The parameters for all scans in this study were a 3D macula scan centered on the fovea covering 6 × 6 mm, resolution 512 × 128, imaging the complete macular area. The instrument utilizes a Fourier domain spectrometer producing cross-sectional B scans and 3-D volumetric images at a speed of 25,000 A scans / sec. OCT scans were used for classification of retinal phenotypes in XLRS using a modified version[21] of Prenner's "Classification scheme for XLRS.10

Mutation Analysis

Blood samples were collected from all participants after obtaining informed consent according to the Helsinki declaration. Genomic DNA was extracted from peripheral blood cells using QIAamp DNA Mini Kit, Qiagen GmbH, Hilden, Germany). *RS1* gene coding regions (exons 1–6) and the flanking intronic sequences were amplified by polymerase chain reaction (PCR) with Platinum Taq DNA polymerase (Invitrogen, Carlsbad, CA, USA) in Peltier Thermal Cycler (BioRad Life Sciences, Hercules, CA, USA). The sequence of the primers and the annealing temperatures set in PCR are listed in Table 5. The amplicons were analyzed on 1.4% agarose gels and stained with ethidium bromide and purified using QIAEX II gel extraction kit (Qiagen) according to the manufacturer's protocol. The purified amplicons were used as sequencing templates. Sequencing was carried out in an ABI3730XL analyzer using Big Dye 3.1 sequencing kit (Applied Biosystems, Foster City, CA, USA). Sequences were assembled and analyzed with Lasergene SeqMan software. The results were compared with the RS1 reference sequence: ENSG00000102104 (http://uswest.ensembl.org/Homo_sapiens/Gene/Summary?db=core;g=ENSG00000102104).

Statistics

Statistical analysis was performed on a computer (SPSS statistical software, ver. 17; SPSS Science, Inc., Chicago, IL). Student's paired t-test was used to evaluate full field ERG and BCVA differences between a patient's eyes as well as differences between same eyes over time. Mann-Whitney U, a non-parametric test for assessing whether two independent samples of observations come from the same distribution was used to compare mfERG data.

RESULTS

Ten patients with clinically diagnosed XLRS were included in this study and were examined at two time points. The first examination was done between ages 6–15 years (mean age 9.3 years) and all the patients were re-examined at the age of 18–25 years (mean age 21.4 years). The mean interval between examinations was 12.1 years (Table 1).

Visual Acuity

Best corrected visual acuity varied in this group of patients but demonstrated no significant difference between a patient's right and left eye at the measured time points (paired student's t-test p=0.64; p=0.116) (Table 2). Comparing BCVA between time points gave a small significance in the left eyes, with better BCVA at the later time point (paired student's t-test p=0.305; p=0.048) (Table 2). At the first time point, there was a positive correlation with age in patients between 6 and 15 years old, (Pearson Correlation 0.531 p=0.016), but at the later time point, when the patients were between 18 and 25 years, there was no correlation found between age and BCVA (Pearson Correlation −0.108 p=0.670) (Figure 1). Visual acuity progresses normally in early childhood and, at age 6 years, virtually 100% of the children in a recent study achieved BCVA 0.5 or better.[22]

Ophthalmologic Examination

Fundus appearances, observed by indirect funduscopy, varied among patients, but all had macular abnormalities at both first and second examination. The fundus findings included a spoke wheel pattern, macular retinoschisis and demonstrated a different degree of retinal changes. Foveal retinoschisis was detected in 6 eyes of 3 patients by funduscopy and OCT, while macular lamellar schisis was visualized by OCT in 12 eyes of 6 patients (Table 1).

Structural and macular dysfunction was further examined with OCT and mfERG (Figure 2, Table 1). Visual field (VF) tests could be assessed at both visits in only seven of the patients, as three of them were too young to co-operate in visual field testing at the first visit. Repeat examination in these seven patients demonstrated results similar to the previous test. The peripheral borders of the visual field tested, with object V:4, was within normal limits in these seven patients at both time-points, while the inner border, tested with object I:4e, demonstrated various degrees of constriction in the visual field.

Full-field ERG

Reduced rod function evaluated by full-field ERG blue light and white bright flash b-wave amplitude was demonstrated in all patients at both ages without any significant difference between the visits (Student's paired t-test bright flash b-wave OD p=0.142 OS p=0.573) or between eyes.

Cone function measured by 30Hz flicker amplitude and implicit time showed a reduction in most of the patients, but there was no significant difference between the two eyes or between visits (Student's paired t-test 30 Hz flicker amplitude OD p=0.981 OS p=0.683, 30 Hz implicit time OD p=0.904 OS p=0.325) (Figure 3 and 4).

A reduced b / a-wave ratio, reflecting a disruption between photoreceptors and second-order neurons, has been a hallmark of x-linked retinoschisis. In all examined patients this ratio was below normal, in average 1.2 ± 0.22 (n=10) at first visit and 1.5 ± 0.65 (n=10) at follow-up visit compared with age matched normal controls 3.5 ± 1.75 (n=30) and 3.3 ± 1.42 (n=34) (Table 3).

Structure and Retinal Function in the Macular Region

Multifocal ERG and OCT—Multifocal ERG measured at the follow-up demonstrated locally subnormal cone function in the macular region in all patients, and significantly delayed implicit time in all ring areas compared with normal controls (Table 4). Optical coherence tomography revealed various degrees of foveal schisis and thinning of the retina in some patients (Table 4, Figure 2), but in some of the patients, there was no schisis-like appearances in the macular or peripheral retina. The 3 patients that exhibited both lamellar and foveal schisis had the lowest mfERG central amplitudes but variable implicit time.

Genetic Analysis—PCR Amplification of the RS1 gene on individual genomic DNA samples with primer sets (Table 5) producing amplicons covering the entire 6 exons with their flanking sequences was carried out in order to identify and confirm the mutations. RS1 mutations were found in three of the nine subjects including a known nonsense mutation in exon 3 (c.120 C>A; p.Cys40X). The C>A substitution changes the actual amino acid from cystiene to a stop codon. As a consequence, the nonsense mutation p.Cys40X produces a nonfunctional truncated RS1 protein (39 amino acid vs. 224 amino acid RS1). This mutation was reported earlier in a Swedish family.3,14 A novel one nucleotide insertion in exon 5 (c. 421_422ins A; pArg141GlnX3) was identified in another patient (Figure 5A). The 1-bp insertion of A residue at nucleotide 421 in exon 5 introduces an amber stop codon, UAG, that prematurely terminates translation—that is, a frame-shift change with Arg 141 as the

first affected amino acid changing to Gln and creating a new reading frame ending in a UAG stop codon at position 3 (pArg141Gln fsX3).

No mutations were detected in the other six patients examined although all coding regions and exon-intron boundaries were sequenced. It is possible that XLRS in these families is caused by a mutation located in the promoter or other regulatory regions including those within introns or unknown splice variants that we didn't detect in this experimental setup. Interestingly, one such intronic mutation was observed in one patient, the atypical T>**C** transversion 35 bp downstream of 5' splice site of intron 3 (c.184 + 35T>C; g.IVS3 + 35T>C; Figure 5B).

In general a majority of splice site mutations involve regions at the positions −2 to +6 at the 5'splice sites and −26 to +1 at the 3'splice sites. Although these positions are more critical for splicing, mutations including point mutations located deep in introns are also known to be associated with diseases.[23,24] The significance of T>C transversion at a distal site from the exon–intron junction in the context of RS1 RNA splicing needs to be further investigated.

DISCUSSION

XLRS is a congenital disease with changes in retinal structure occurring early in life. There are currently no proven treatments for this human disease, but recent reports of improved retinal structure and function after gene transfer therapy in mouse retinoschisin knockout models of XLRS[30,32,33] are promising. One important aspect of successful retinal rescue is almost certainly the necessity of early treatment before any major structural damage has occurred. Considering the relative stability of visual function, or even slight increase in function, possibly the result of slow maturation, shown for the age group in this study, this might be a good period for intervention in the disease process, eg, with aav-*RS1* gene therapy.

Previous studies have defined X-linked juvenile retinoschisis (XLRS) as a neuro-developmental abnormality caused by retinoschisin gene mutations characterized by a splitting of the retina leading to visual failure early in life. The phenotype has therefore been well characterized but rather few studies have investigated the rate of progression according to changes of function and structure of the retina in the macular region.

Forsius[25] evaluated the visual acuity in 183 Finnish patients and found that, after an early decrease in visual acuity, it seems to be stable for many years. Comparable results have been published[13,15,26] demonstrating no changes in visual acuity after childhood, and therefore, XLRS has been considered to be a slowly progressive retinal degeneration. In the present longitudinal study, examining XLRS patients at early ages with a follow-up 12 years later, result for visual acuity were similar with no significant differences between the eyes at the two different time points.

Electrophysiological examination has been of major interest in XLRS patients, as the disproportionate reduction in the b-wave reflects the site of dysfunction. The change of the ERG traces with altered b / a wave ratio and reduced amplitude and prolonged implicit time for the 30Hz flicker stimulation[13,15] has been of diagnostic value for this disorder.

Since the RS-gene was identified as the disease causing gene, other phenotypes with atypical ERG findings have also been recognized during recent years,[14, 27–29] confirming the variety of phenotypes in XLRS patients. In the present study on patients of similar age, the ERG results confirm this phenotypic variation and showed it remained stable during the 12 year follow-up time period. Few previous studies have evaluated the rate of progression[15]

of the XLRS disorder by retinal function. In the present study the amplitude reflecting the cone and rod response did not demonstrate any progression during a follow-up period of 12 years after childhood. This is in consistent with previous studies that show that this disorder progresses during early childhood and thereafter is stable over a long period of time.[25] Though not significant, there was a tendency towards increased b-wave amplitudes and increased b / a-wave ratio at the later time point reflecting a possible late visual maturation. This has been suggested in a knockout mouse model for X-linked retinoschisis.[30]

Five of the 10 patients in this study belong to two families both living within a small region in southern Sweden, and there is a convincing possibility that they have the same ancestor. An XLRS mutation in the exons could not be found in these patients, but it is possible that there is a mutation within the promoter or in the introns. Clinically, they exhibit blunt macular reflex, an x-linked inheritance pattern, a reduced b / a-wave ratio and a reduced rod response with a relatively spared cone function, which would distinguish it from other congenital degenerations such as X-linked congenital stationary night blindness (CSNB).

Three different mutations were detected in these nine patients, including a previously reported nonsense mutation in exon 3, a novel insertion in exon 5 and a novel intronic mutation at 5' splice site of intron 3. The significance of this intronic mutation as well as the probability of detecting other mutation in the same patient needs to be further investigated, but in this patient, it caused phenotypical juvenile retinoschisis.

The majority of young patients with XLRS exhibit a wheel-like cystic formation across the macula region, whereas middle-aged and older patients more often present a non-specific atrophic appearance of the macula.[15] With new methods, including OCT, more extensive evaluation of these structural changes in the macular region has been done.[28] In the present study of young patients, OCT demonstrated a variety of cystic formations and degeneration. Recent reports have confirmed phenotypic variations in the fundus appearance as well, in some case without any typical schisis cavities in young patients.[28,29] The present study showed that the progress of degeneration in these structures also is extremely slow. These findings concur with a previous study that visual acuity is stable during this period if no secondary retinal event such as retinal detachment or vitreal hemorrhage occurs.[15]

These structural changes in the macular region could be correlated to local dysfunction by use of the multifocal ERG.[27,31] In the present study, reduced perifoveal function was seen in all patients, even without OCT verified schisis cavities. This could be due to small inner retinal synaptic disruptions not detectable by OCT. Though no statistics were done, because of the small sample size, the three patients with both lamellar and foveal schisis had more affected central function with lower amplitudes suggesting a correlation between schisis cavities and central retinal function.

Clinical follow-up of young XLRS patients with different genotypes did not indicate a progression of the retinal dysfunction after early childhood. MfERG and OCT demonstrated a wide variety of structural and functional macular changes at the follow-up.

Acknowledgments

We thank Ing-Marie Holst and Boel Nilsson for skillful technical assistance. This study was supported by grants from Stiftelsen Synfrämjandets Forskningsfond, the Swedish Medical Research Council (projects no. 2007–3385), the Foundation Fighting Blindness, Owings Mills, Maryland, USA and NIH Grant Z01-DC000065

REFERENCES

1. George ND, Yates JR, Moore AT. X linked retinoschisis. The British Journal of Ophthalmology 1995;79:697–702. [PubMed: 7662639]
2. Sauer CG, Gehrig A, Warneke-Wittstock R, et al. Positional cloning of the gene associated with X-linked juvenile retinoschisis. Nature Genetics 1997;17:164–170. [PubMed: 9326935]
3. The Retinoschisis C. Functional implications of the spectrum of mutations found in 234 cases with X-linked juvenile retinoschisis. The Retinoschisis Consortium. Human Molecular Genetics 1998;7:1185–1192. [PubMed: 9618178]
4. Takada Y, Fariss RN, Tanikawa A, et al. A retinal neuronal developmental wave of retinoschisin expression begins in ganglion cells during layer formation. Investigative Ophthalmology & Visual Science 2004;45:3302–3312. [PubMed: 15326155]
5. Takada Y, Fariss RN, Muller M, et al. Retinoschisin expression and localization in rodent and human pineal and consequences of mouse RS1 gene knockout. Molecular Vision 2006;12:1108–1116. [PubMed: 17093404]
6. Vogel W. Discoidin domain receptors: structural relations and functional implications. FASEB Journal 1999;13 Suppl:S77–S82. [PubMed: 10352148]
7. Wu WW, Wong JP, Kast J, et al. RS1, a discoidin domain-containing retinal cell adhesion protein associated with X-linked retinoschisis, exists as a novel disulfide-linked octamer. Journal of Biological Chemistry 2005;280:10721–10730. [PubMed: 15644328]
8. Eksandh LC, Ponjavic V, Ayyagari R, et al. Phenotypic expression of juvenile X-linked retinoschisis in Swedish families with different mutations in the XLRS1 gene. Archives of Ophthalmology 2000;118:1098–1104. [PubMed: 10922205]
9. Gass, JDM. Stereoscopic Atlas of Macular Diseases. 3 ed.. St Louis: Mosby; 1987.
10. Prenner JL, Capone A Jr, Ciaccia S, et al. Congenital X-linked retinoschisis classification system. Retina 2006;26:S61–S64. [PubMed: 16946682]
11. Gerth C, Zawadzki RJ, Werner JS, et al. Retinal morphological changes of patients with X-linked retinoschisis evaluated by Fourier-domain optical coherence tomography. Archives of Ophthalmology 2008;126:807–811. [PubMed: 18541843]
12. Peachey NS, Fishman GA, Derlacki DJ, et al. Psychophysical and electroretinographic findings in X-linked juvenile retinoschisis. Archives of Ophthalmology 1987;105:513–516. [PubMed: 3566604]
13. Deutman, AF. The hereditary dystrophies of the posterior pole of the eye. Assen: Van Gorcum; 1971. p. 484
14. Eksandh LC, Ponjavic V, Ayyagari R, et al. Phenotypic expression of juvenile X-linked retinoschisis in Swedish families with different mutations in the XLRS1 gene. Archives of Ophthalmology 2000;118:1098–1104. [PubMed: 10922205]
15. Kellner U, Brummer S, Foerster MH, et al. X-linked congenital retinoschisis. Graefes Archives for Clinical and Experimental Ophthalmology 1990;228:432–437.
16. Tantri A, Vrabec TR, Cu-Unjieng A, et al. X-linked retinoschisis: a clinical and molecular genetic review. Survey of Ophthalmology 2004;49:214–230. [PubMed: 14998693]
17. Marmor MF, Fulton AB, Holder GE, et al. ISCEV Standard for full-field clinical electroretinography (2008 update). Documenta Ophthalmologica 2009;118:69–77. [PubMed: 19030905]
18. Bearse JMA, Sutter EE. Imaging localized retinal dysfunction with the multifocal electroretinogram. Journal of the Optical Society of America A 1996;13:634–640.
19. Sutter EE, Tran D. The field topography of ERG components in man—I. The photopic luminance response. Vision Research 1992;32:433. [PubMed: 1604830]
20. Hood DC, Bach M, Brigell M, et al. ISCEV guidelines for clinical multifocal electroretinography. Documenta Ophthalmologica 2008;116:1–11. (2007 edition). [PubMed: 17972125]
21. Lesch B, Szabo V, Kanya M, et al. Clinical and genetic findings in Hungarian patients with X-linked juvenile retinoschisis. Molecular Vision 2008;14:2321–2332. [PubMed: 19093009]

22. Pan Y, Tarczy-Hornoch K, Cotter SA, et al. Visual acuity norms in pre-school children: the Multi-Ethnic Pediatric Eye Disease Study. Optometry & Vision Science 2009;86:607–612. [PubMed: 19430325]

23. Dehainault C, Michaux D, Pagès-Berhouet S, et al. A deep intronic mutation in the RB1 gene leads to intronic sequence exonisation. European Journal of Human Genetics 2007;15:473–477. [PubMed: 17299438]

24. Harland M, Mistry S, Bishop DT, et al. A deep intronic mutation in CDKN2A is associated with disease in a subset of melanoma pedigrees. Human Molecular Genetics 2001;10:2679. [PubMed: 11726555]

25. Forsius H, Krause U, Helve J, et al. Visual acuity in 183 cases of X-chromosomal retinoschisis. Canadian Journal of Ophthalmology 1973;8:385–393. [PubMed: 4742888]

26. Bengtsson B, Linder B. Sex-linked hereditary juvenile retinoschisis: presentation of two affected families. Acta Ophthalmologica (Copenh) 1967;45:411–423.

27. Eksandh L, Andreasson S, Abrahamson M. Juvenile X-linked retinoschisis with normal scotopic b-wave in the electroretinogram at an early stage of the disease. Ophthalmic Genetics 2005;26:111–117. [PubMed: 16272055]

28. Renner AB, Kellner U, Fiebig B, et al. ERG variability in X-linked congenital retinoschisis patients with mutations in the RS1 gene and the diagnostic importance of fundus autofluorescence and OCT. Documenta Ophthalmologica 2008;116:97–109. [PubMed: 17987333]

29. Robson AG, Mengher LS, Tan MH, et al. An unusual fundus phenotype of inner retinal sheen in X-linked retinoschisis. Eye (London) 2009;23:1876–1878.

30. Kjellstrom S, Bush RA, Zeng Y, et al. Retinoschisin gene therapy and natural history in the Rs1h-KO mouse: long-term rescue from retinal degeneration. Investigative Ophthalmology & Visual Science 2007;48:3837–3845. [PubMed: 17652759]

31. Robson AG, Michaelides M, Saihan Z, et al. Functional characteristics of patients with retinal dystrophy that manifest abnormal parafoveal annuli of high density fundus auto-fluorescence; a review and update. Documenta Ophthalmologica 2008;116:79–89. [PubMed: 17985165]

32. Zeng Y, Takada Y, Kjellstrom S, et al. RS-1 Gene delivery to an adult Rs1h knockout mouse model restores ERG b-wave with reversal of the electronegative waveform of X-linked retinoschisis. Investigative Ophthalmology & Visual Science 2004;45:3279–3285. [PubMed: 15326152]

33. Min SH, Molday LL, Seeliger MW, et al. Prolonged recovery of retinal structure/function after gene therapy in an Rs1h-deficient mouse model of x-linked juvenile retinoschisis. Molecular Therapy 2005;12:644–651. [PubMed: 16027044]

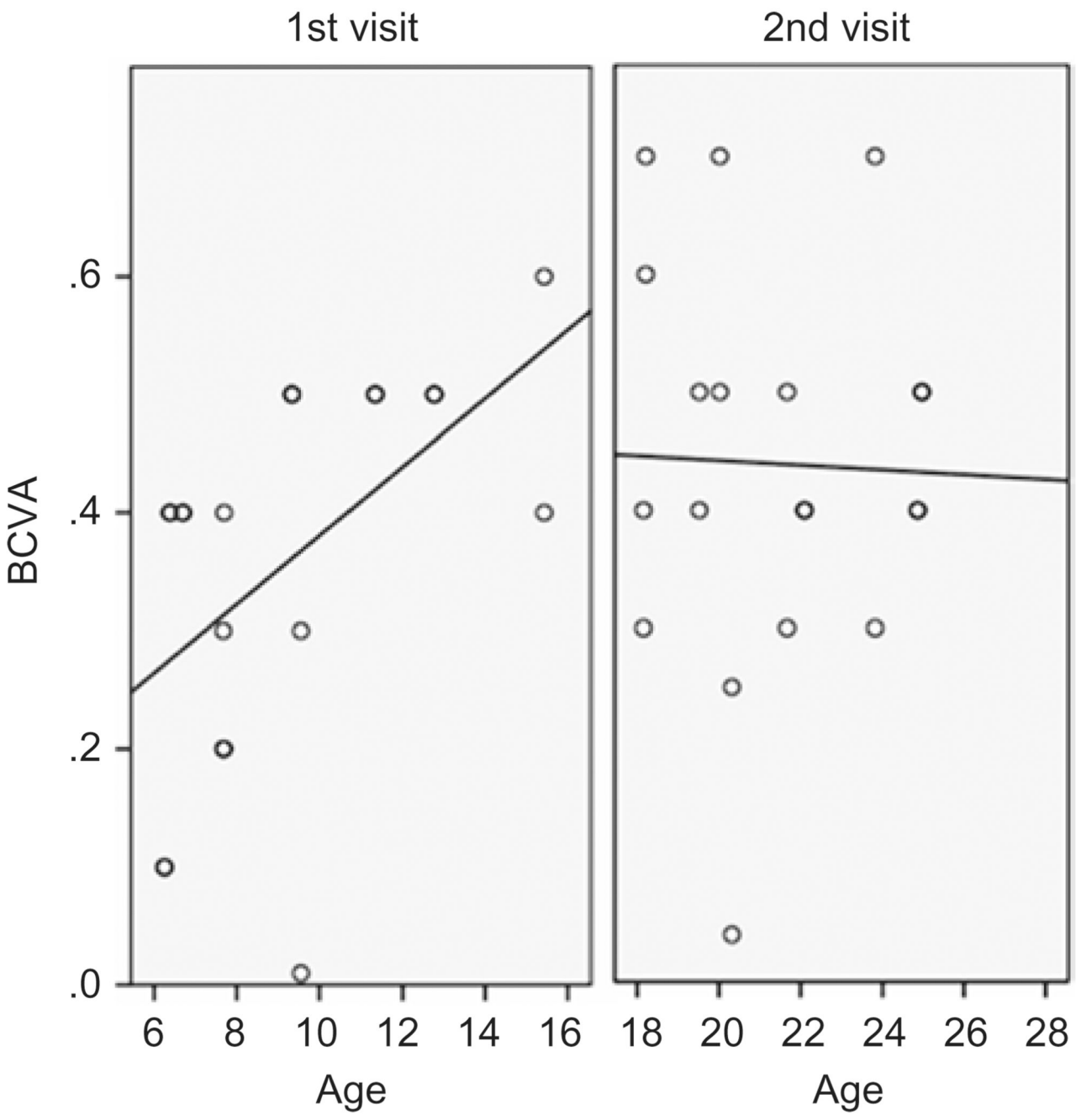

FIGURE 1.
Best corrected visual acuity (BCVA)(Snellen) at 1st and 2nd visit plotted against age (years) at examination. Regression line at 1st visit with positive correlation with age (Pearson Correlation 0.531 p=0.016), at 2nd visit no correlation (Pearson Correlation −0.108 p=0.670).

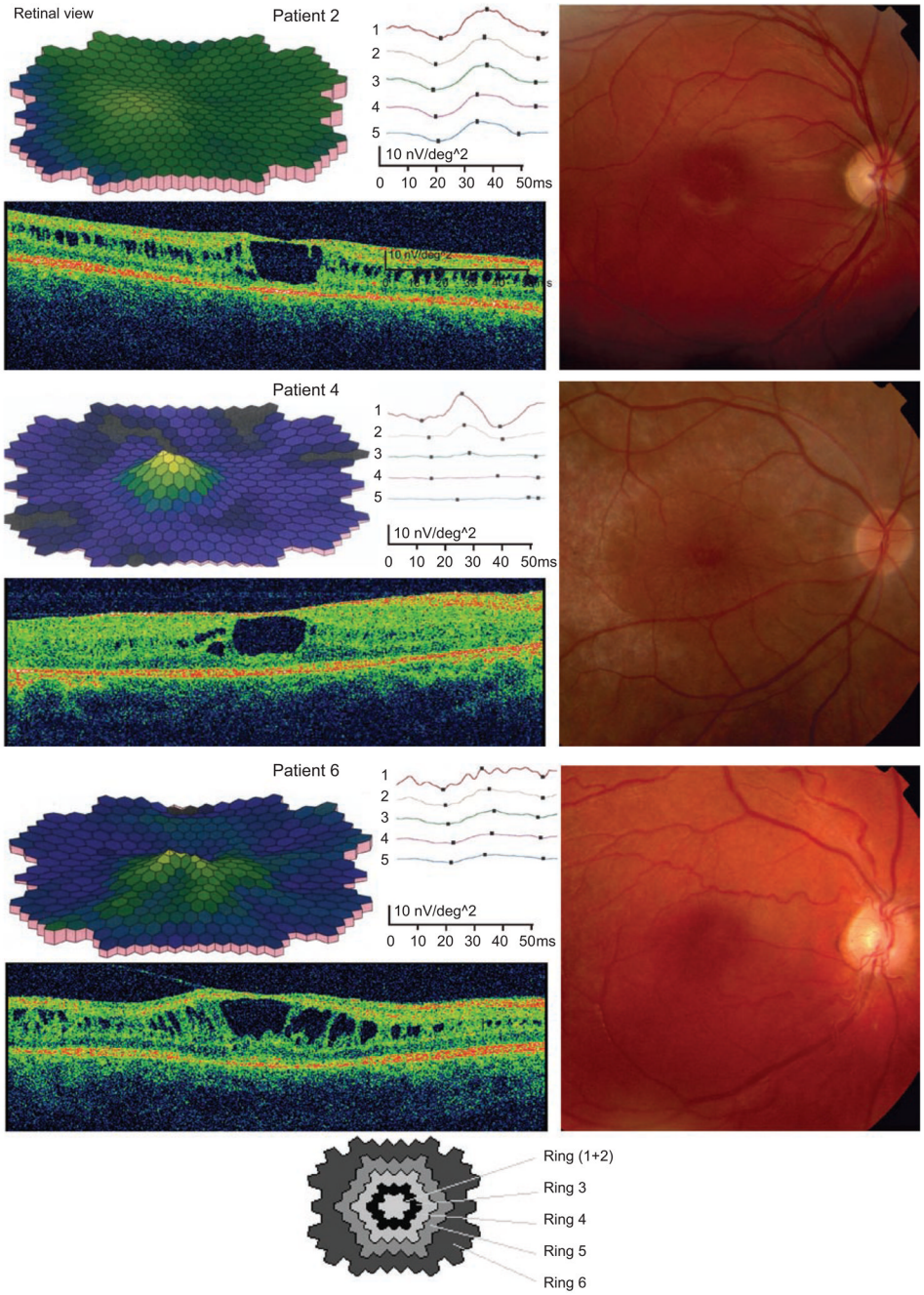

FIGURE 2.

Box plot of full field ERG measurements from both eyes at 1st and 2nd visit compared with normal ERG (18–25 years old n=10). (a) 30Hz flicker amplitude (μV). (b) White bright flash b-wave amplitude (μV). (c) 30Hz flicker implicit time (ms). (d) Calculated b / a-wave ratio on right eyes. Outliers are marked with a circle and extreme cases with an asterisk.

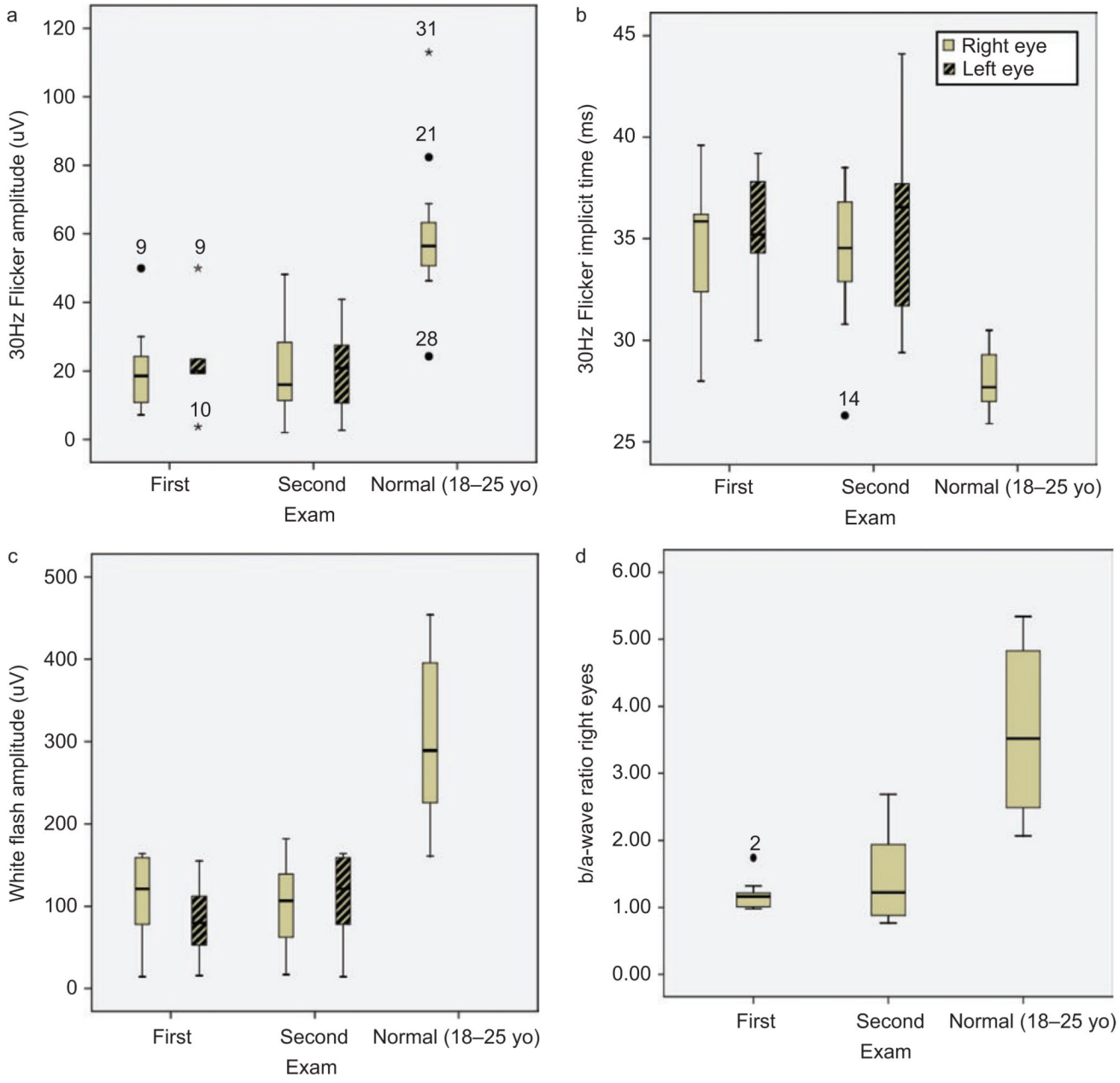

FIGURE 3.

Decreased macula function (multifocal electroretinography) and structural alteration with foveal and lamellar retinoschisis (Fundus image and optical coherence tomography) at last visit (3 cases).

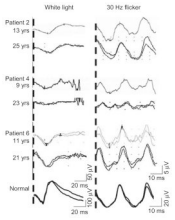

FIGURE 4.

Full-field electroretinography traces at 1st and 2nd visit (3 cases). White light as a measurement of mixed rod cone function and 30 Hz flicker as a measurement of cone function. Note different scale for normal ERG traces.

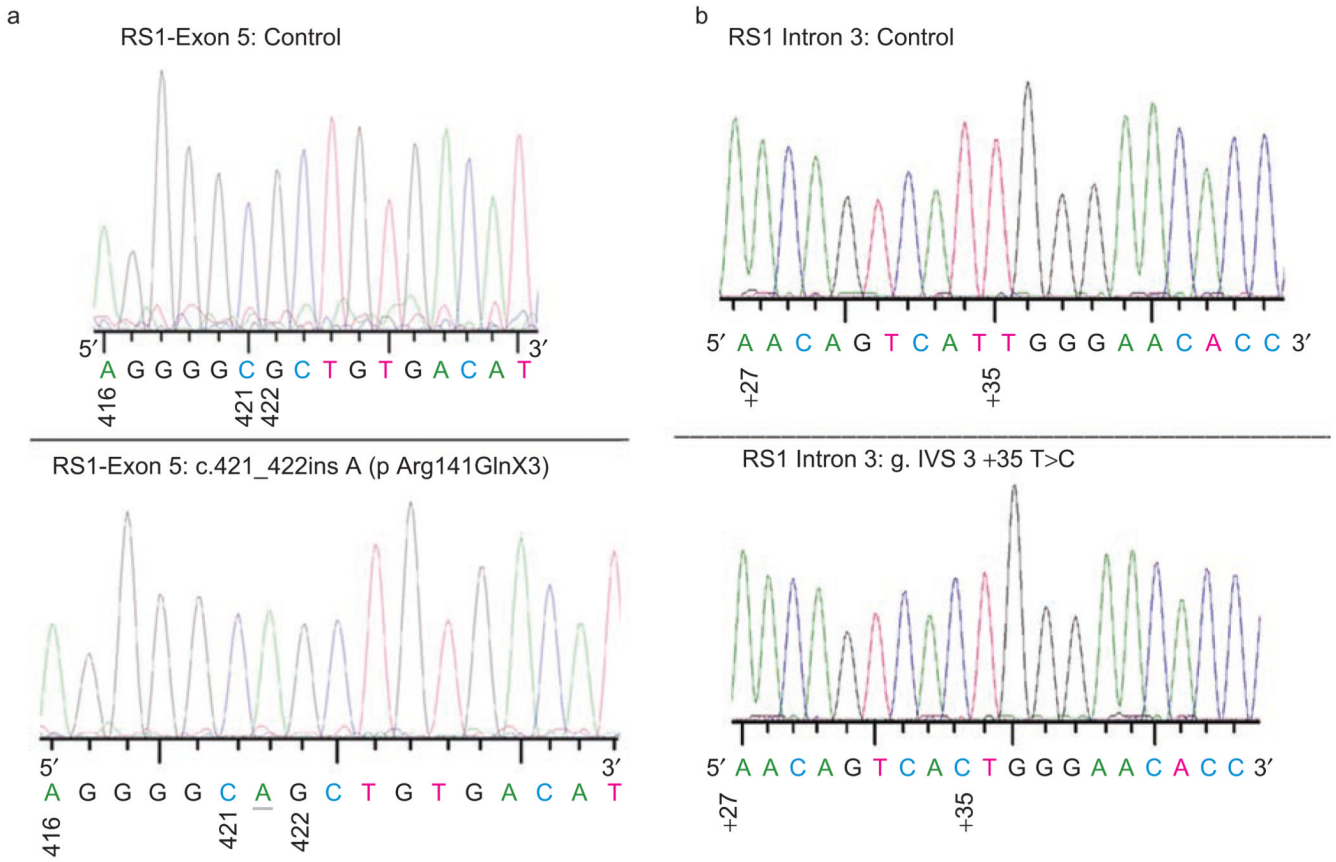

FIGURE 5.

Sequence chromatograms showing the (a) insertion mutation in exon 5 {c.421_422 ins A (p Arg141GlnX3)}. Mutation was numbered according to Gene Bank NM_000330. Nucleotide 1 is A of the ATG initiation codon (CDS 36–710). (b) T>C transversion in intron 3 of *RS1* gene. The genomic reference sequence is ENSG00000102104. The mutation was numbered the following way: the number of the last nucleotide of preceding exon 3 (=nt 184) and a plus sign and the position of T in intron(+35) which is **c.184 + 35T>C**. Description of the same mutation in the earlier format: (g.IVS3 + 35T>C). The normal sequences from the corresponding region are also shown in the upper panel.

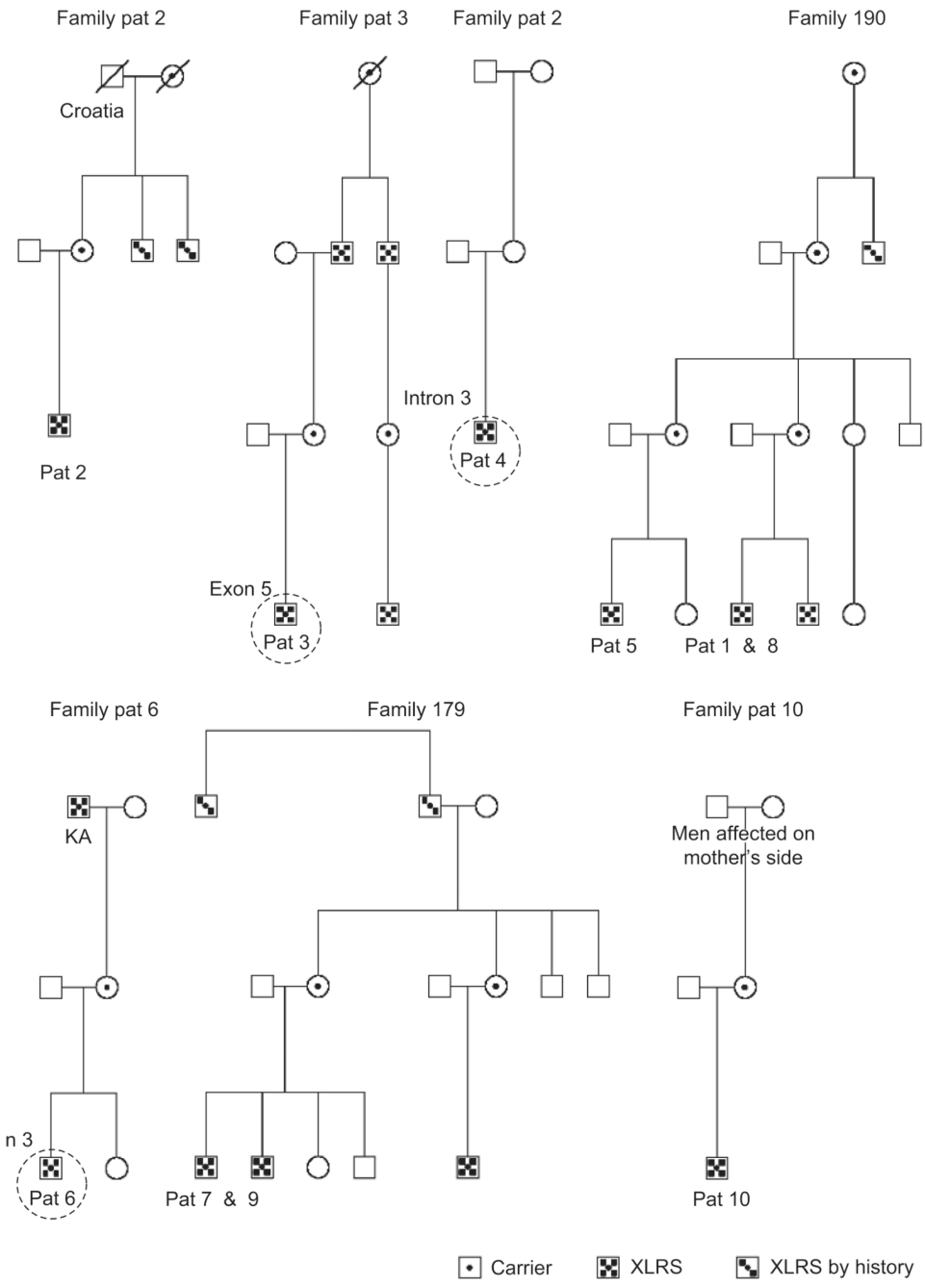

FIGURE 6.

Pedigree of patients. Members from family 190 and family 179 previously examined. Circles indicate found mutations in this study.

TABLE 1

Table showing patient details: age at 1st and 2nd visit, location of mutations, heredity and family origin and retinal schisis phenotype (modified classification scheme of XLRS by Prenner et. al., 2006 [Ref. 10])

Patient no	Age 1st visit (years)	Age 2st visit (years)	Follow up time (years)	Mutation	Effect of mutation	Localization	Hereditary. Swedish RP registry	Phenotype' OD/OS		Family origin
1	11.8	25	13.4				190	–	–	Southeast Sweden
2	12.8	24.9	12.1	Samples not taken because of patient			2 uncles on mother side	3	3	Middle Part of Sweden
3	16.1	23.8	7.7	c421_422ins A	p.Arg 14 1G InX3	exon5	Yes	2	2	Middle Part of Sweden
4	9.4	22.1	12.7	c.184 + 35T>C	Frameshift truncated protien?	intron3	No	3	3	Middle pert of Sweden
5	7.7	21.7	14				190	2	2	Southeast Sweden
6	9.6	30.3	10.7	c.120 C>A	p.Cys40X Premature termination	exon 3	240	3	3	Southeast Sweden
7	7.7	19.5	11.8				179	2	2	Southeast Sweden
8	8	20	14				190	–	–	Southeast Sweden
9	6.4	18.2	11.8				179	–	–	Southeast Sweden
10	6.3	18.2	11.9				Men on nnother side	–	–	Middle part of Sweden

XLRS form	Type	Foveal cystic sc hi sis (clinical and OCT exam)	Macular lamellar schlsls (OCT exam)	Peripheral schl sis (clinical exam)
Cystic	Type 1 Feveal	+		
	Type 2 Lamellar		+	
	Type 3 Foveolamcllar	+	+	
	Typo 4 Complex	+	+	+
	Tvpe-Ti Fovcopcriphcral	+	–	+
	Type 6 Peripheral	–	–	+
Atrophic	Type 7 Nonspecific	–	–	–

TClassification scheme of XLRS modified Premier as published

TABLE 2

Inter-ocular visual changes at different time points. Best corrected visual acuity (BCVA) (OD right eye, OS left eye). Student's paired t-test

	Paired Student's t-test BCVA between eyes				
Time point	**Eye**	**Mean**	**N**	**Std. Deviation**	**Sig. (2-tailed)**
1st	OD	0.35	10	0.14	0.640
	OS	0.37	10	0.19	
2nd	OD	0.40	10	0.11	0.115
	OS	0.48	10	0.20	
	Paired Student's t-test BCVA between time points				
Eye	Time point	Mean	N	Std. Deviation	Sig. (2-tailed)
OD	1st	0.35	10	0.143	0.305
	2nd	0.40	10	0.112	
OS	1st	0.37	10	0.187	0.049*
	2nd	0.48	10	0.200	

BCVA: Best corrected visual acuity; Std: Standard;

TABLE 3

Full-field ERG measurements from right eyes at 1st and 2nd visit. White bright flash b-wave amplitude (μV), calculated b/a-wave ratio, 30Hz flicker amplitude (μV), 30Hz flicker implicit time (ms), Age matched normal, (1st visit 6–15 years, n= 30, mean =10.1y SD=2.5; 2nd 15–30 years, n=36, mean 21.8y, SD=4.9)

	White amp (μV)		b/a ratio		30Hz flick amp (μV)		30 Hz flick imp (ms)	
Patient	**1st**	**2nd**	**1st**	**2nd**	**1st**	**2nd**	**1st**	**2nd**
1	122	164	1.22	2.15	24	28	36	37
2	87	161	1.74	1.79	19	23	33	32
3	148	125	1.32	1.26	20	24	36	35
4	48	14	1.20	0.88	19	3	40	44
5	96	159	1.20	1.94	15	19	36	37
6	59	78	1.01	0.77	7	11	32	40
7	45	99	1.00	1.03	30	40	28	29
8	51	145	1.13	2.69	10	11	36	38
9	80	68	1.07	0.88	50	41	30	31
10	12	117	0.98	1.19	11	11	38	36
Mean	74.7	113.0	1.19	1.46	20.4	20.9	34.5	35.9
SD	40.3	48.8	0.22	0.65	12.5	12.7	3.6	4.4
Normal	315.7	311	3.51	3.34	55.2	59.7	28.8	28.4
SD (n=30/34)	86	92.3	1.75	1.42	26.9	23.6	1.7	1.4

TABLE 4

Multifocal electroretinography (mfERG) measurements from right eyes at 2nd visit including best corrected visual acuity (BCVA) and retinal schisis phenotype (modified classification scheme of XLRS by Prenner). (Normal controls n=30 eyes from 21 patients; mean: 38.2y SD=11.9). Mann-Whitney U, a non-parametric test for assessing whether two independent samples of observations come from the same distribution, was calculated

Pat	R1 lat	R1 amp	R2 lat	R2 amp	R3 lat	R3 amp	R4 lat	R4 amp	R5 lat	R5 amp	BCVA OD	Schisis ODT
1	30	30,6	29,2	16,8	28,3	12,4	30	8,9	30,8	8,3	0.5	-
2	34,2	13,7	33,3	12,6	34,2	11,6	30,8	10,5	30,8	9,3	0.4	3
3	34,2	18,9	33,3	13,1	31,7	10,4	31,7	10,1	32,5	11	0.3	2
4	25,8	15,7	26,7	7,1	28,3	2,6	38,3	1,2	49,2	1,2	0.4	3
5	29,2	27	30	13,9	31,7	8,6	35,8	6,2	35,8	6	0.3	2
6	29,2	12,6	31,7	9,9	33,3	7,9	32,5	5,6	30	4,8	0.25	3
7	33,3	26,5	31,7	18,1	31,7	13,9	31,7	12,1	29,2	12,3	0.4	2
8	30	22	29,2	15	28,3	9,3	29,2	7,5	30	7	0.5	-
9	30,8	52,2	30	34,9	30	25,7	30,8	23	30,8	21,5	0.6	-
10	29,2	20,5	29,2	13,4	30	8,7	30	5,7	31,7	8,2	0.3	-
Mean	*30,6*	*24*	*30,4*	*15,5*	*30,8*	*11,1*	*32,1*	*9,1*	*33,1*	*9*	*0.40*	
Normals	*27*	*32*	*26.2*	*22.4*	*25.7*	*18.2*	*25.9*	*16.1*	*26.3*	*15.7*	*1.0*	
SD	*3*	*11.9*	*1.45*	*7.25*	*1.45*	*5.4*	*1.45*	*4.55*	*1.5*	*4.6*	*0.1*	
P value	0.000	0.011	0.000	0.001	0.000	0.000	0.000	0.000	0.000	0.000		

TABLE 5

The sequence of the primers and the annealing temperatures set in PCR for amplification of RS1 coding exons and the flanking intron sequences from genomic DNA samples

Name of Primer	Sequence	Ta(°C)
RS1 exon 1 F	5'-CTTCCATGAGACTTCCTTGTTGAG-3'	55
RS1 exon 1 R	5'-ATTTCTGAGACCCATCCTGTTTTC-3'	
RS1 exon 2 F	5'-gtgatgctgttggatttctc-3'	55
RS1 exon 2 R	5'-gtcctctatgttattttggc-3'	
RS1 exon 3 F	5'-ACAGTTGCCTTTGACCGTGAC-3'	63
RS1 exon 3 R	5'-GAAGCAGGGGCCATTGTGAGA-3'	
RS1 exon 4 F	5'-ggtgcttgttgagtattgag-3'	55
RS1 exon 4 R	5'-aaaatccccgggccctgc-3'	
RS1 exon 5 F	5'-ATGCAGGGAGAGGGAGAATGAGATG-3'	63
RS1 exon 5 R	5'-CACCAAAGCAAGCCCAGGAAAGAGA-3'	
RS1 exon 6 F	5'-Cccgatgtgatggtgacagg-3'	62
RS1 exon 6 R	5'-ctttgttctgactttctctggc-3'	

PCR conditions: 94°C 4 min; 30 cycles of 94°C 30s, Ta 30s, 72°C 30s, 72°C 5min. (Ta: annealing temperature).